NMR Conformational Analysis and Theoretical Calculations for 2-Aryl-1,3-dihydroxy-4,4,5,5-tetramethylimidazolidines

by **Antônio F. De C. Alcântara**[a]), **Maria G. F. Vaz**[c]), **Humberto O. Stumpf**[c]), **Dorila Piló-Veloso**[c]), and **Wagner B. De Almeida***[b])[c])

[a]) Departamento de Química, ICE, and [b]) Laboratório de Química Computacional e Modelagem Molecular (LQC-MM), Universidade Federal do Amazonas, Campus Universitário, Manaus-AM, CEP 69078-000, Brasil
[c]) Departamento de Química, ICEx, Universidade Federal de Minas Gerais, Belo Horizonte-MG, CEP 31270-901, Brasil
(e-mail: wagner@netuno.qui.ufmg.br)

Conformational studies of 1,3-dihydroxy-4,4,5,5-tetramethyl-2-(pyridin-1-yl)imidazolidine (**1a**) and 1,3-dihydroxy-4,4,5,5-tetramethyl-2-(pyridin-3-yl)imidazolidine (**1b**), carried out by using 1D ^{1}H- and ^{13}C-NMR and 2D HMQC, HMBC, and NOESY experiments and with the aid of theoretical calculations, indicate that the OH groups are *trans* to the pyridinyl substituent. Because the two ^{1}H-NMR signals of the Me groups are distinguishable and do not change between 290 and 380 K, it is proposed that **1a** and **1b** have each only one conformation in this temperature range. This behavior was not found with 1,3-dihydroxy-4,4,5,5-tetramethyl-2-(pyridin-2-yl)imidazolidine (**1c**) because its Me ^{1}H-NMR signals cross over at 300 K. Hence, more than one conformation must be present, beyond those produced by simple inversions. Theoretical calculations including temperature and solvent effects were performed to provide further information on the conformational analysis and to help to assign the NMR data. The combination of NMR measurements and quantum-chemical calculations is shown to be a very promising strategy for conformational analysis studies in solution.

1. Introduction. – The 1,3-dihydroxy-4,4,5,5-tetramethyl-2-pyridinylimidazolidines have been used in molecular-magnetism studies [1]. In previous work, a conformational study based on ^{1}H- and ^{13}C-NMR and semi-empirical calculations of 1,3-dihydroxy-4,4,5,5-tetramethyl-2-(pyridin-4-yl)imidazolidine (**1a**), 1,3-dihydroxy-4,4,5,5-tetramethyl-2-(pyridin-3-yl)imidazolidine (**1b**), and 1,3-dihydroxy-4,4,5,5-tetramethyl-2-(pyridin-2-yl)imidazolidine **1c** was carried out [2] (*Fig. 1*). This work proposed that all three imidazolidines probably have the same general conformation, with the Me groups in axial and equatorial positions and both OH groups *trans* to the pyridinyl substituent, regardless of the position of free valency at the pyridinyl substituent. Furthermore, the results suggested that the axial Me C-atoms lie relatively closer to the O(γ) atoms, contributing to a significant increase in electronic density, for all three pyridinyl substituents. Diamagnetic shielding significantly influences the ^{1}H- and ^{13}C-NMR chemical shifts of the Me groups. As a consequence, the signals with the smaller δ(C) and the larger δ(H) can be assigned to the axial Me groups, and *vice versa* for the equatorial Me groups.

In this work, we attempt to explain how the δ(H) and δ(C) vary both with temperature and with the structure of the pyridinyl substituent, and to relate this to conformational changes in the three imidazolidines **1**. NOESY Data, quantum-chemical calculations, including thermal and solvent contributions to the relative

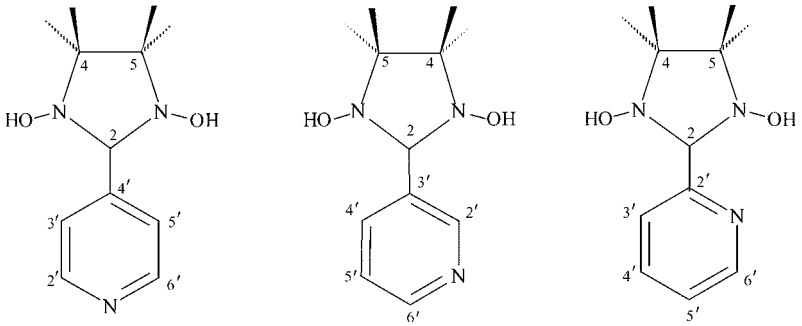

1a **1b** **1c**

Fig. 1. *1,3-Dihydroxy-4,4,5,5-tetramethyl-2-pyridinyl-imidazolidines* **1**

conformational energies, and the effect of the OH groups on the chemical shifts of the Me groups are reported.

2. Experimental. – The syntheses of **1** were carried out according to the methodology described previously [2], where the yields and properties (m.p.s., elemental analyses, ^{1}H- and ^{13}C-NMR, and IR spectra) have been reported. ^{1}H- and ^{13}C-NMR Spectra: *Bruker 400-Avance* spectrometer; in (D_6)DMSO; chemical shifts δ in ppm rel. to $SiMe_4$ as internal standard, and scalar coupling constants J in Hz; ^{1}H-NMR; dwell time (DW) 121.600 μs, acquisition time (AQ) 3.985 s, number of transients (NS) 16, recycle delay (RD) 1.000 s; ^{13}C-NMR DW 15.700 μs, AQ 1.029 s, NS 323, RD 2.000 s, decoupling multiple resonance method *Waltz-16*; HMQC and HMBC: 121.800 μs, AQ 0.511 s, NS 16, RD 2.000 s, delay for long-range coupling (D6) 0.070 s, TD 4096 (F_2) and 256 (F_1); NOESY: DW 305.600 μs, AQ 0.626 s, NS 16, RD 2.000 s, mixing 200 ms, time evolution 3 μs, TD 2048 (F_2) and 512 (F_1). The NMR spectra were calculated for the three isomers **1** with the *ACD/Labs* (version software) [3] program.

3. Calculation. – The spatial arrangement of the substituent groups at the imidazolidine ring suggested by the NOESY experiment were used as initial models for energy-minimization calculations in the gas phase. Geometry optimizations were initially carried out by using the *Hartree-Fock* (HF) and density-functional theory (DFT) [4], with the BLYP [5] functional and the 6-31G(d) basis set [6] as implemented in the TITAN [7] program. A complete search for stationary points on the potential-energy surface (PES), including rotations of the pyridinyl group, were accomplished at the HF level of theory employing the 3-21G(d) [8], by using the geometries previously obtained as the starting point and by employing the Gaussian-98 [9] suite of programs. All of these fully optimized structures were characterized as true minimum energy on the PES through frequency calculations (when all frequencies are real, this corresponds to a true minimum-energy structure). The energetically plausible structures found for **1a**–**c** were further fully re-optimized at the HF-6-31G(d) level of theory, which is our best computationally feasible approach for geometry optimization with Gaussian-98 [9]. Electron-correlation effects were included in the last stage of the calculations through single-point-energy calculations by using the *Møller–Plesset* second-order perturbation theory (MP2) [10] with the improved 6-31G(d,p) basis set (including polarization functions on all atoms) for the HF/6-31G* fully optimized geometries. The temperature effect was evaluated by calculation of the thermal-energy correction (ΔG_T) to the electronic-plus nuclear-repulsion-energy difference ($\Delta E^{gas}_{ele\text{-}nuc}$) by using well-known formulas of statistical thermodynamics [11–13]. The solvent effect (DMSO, ε 46.7) was assessed with the continuum PCM (polarizable continuum model) [14] as implemented in the *ab initio* Gaussian-98 package [9]. The solvation *Gibbs* energies were evaluated by the well-known thermodynamic cycle [15], where the *Gibbs* energy differences in solution (ΔG^{sol}) are obtained from the sum of two contributions: a gas-phase energy (ΔG^{gas}), calculated from $\Delta E^{gas}_{ele\text{-}nuc}$ plus ΔG_T, and a solvation energy term (ΔE^{solv}), calculated with the continuum approach (*Eqn. 1*). The ΔG_T and ΔE^{solv} terms were evaluated at the HF/6-31G(d) level of theory. MP2/6-31G(d,p)//HF/6-31G(d) Calculations were also performed and are reported. The double slash means that single-point-solvation-energy calculations are evaluated at the fully optimized HF/6-31G(d) geometry. The electronic counterpart ($\Delta E^{gas}_{ele\text{-}nuc}$) was

calculated at the correlated level of theory MP2/6-31G(d,p) as a single-point-energy calculation at the HF/6-31G(d) geometry, a procedure that has been shown to work very well for chemical reactions in solution [16].

$$\Delta G^{sol} = \Delta G^{gas} + \Delta E^{solv} = \Delta E^{gas}{}_{elec\text{-}nuc} + \Delta G_T + \Delta E^{solv} \quad (1)$$

4. Results and Discussion. – The assignments of the ^{1}H- and ^{13}C-NMR data of **1a** and **1b** at 300 K were confirmed by the correlations obtained from HMQC, and also from HMBC and NOESY experiments (*Tables 1* and *2*). The NMR signals of these compounds did not vary significantly with temperature between 290 and 380 K. The OH *s* at δ(H) 7.96 in the spectrum of **1a** and at δ(H) 7.89 in that of **1b** indicates that, in these cases, the OH groups remain in a constant chemical environment. Also, NOESY correlations between the two OH and H–C(2) show that all these are on the same side of the imidazolidine ring.

Table 1. *^{1}H- and ^{13}C-NMR Chemical Shifts for* **1a** *at 300 K, Including HMQC* (^1J(C,H)), *HMBC* (^nJ(C,H), n = 2, 3), *and NOESY Correlations.* In (D_6)DMSO.

	HMQC		HMBC		NOESY
	δ(C)	δ(H)	^2J(C,H)	^3J(C,H)	^{1}H,^{1}H
H–C(2)	89.1	4.53	–	7.96; 7.48	1.09; 7.48; 7.96
C(4), C(5)	66.5	–	1.03; 1.09	1.03; 1.09	–
C(4′)	150.7	–	–	8.52	–
H–C(3′), H–C(5′)	123.4	7.48	8.52	7.48; 4.53	1.03; 4.53; 7.96; 8.52
H–C(2′), H–C(6′)	149.1	8.52	7.48	8.52	7.48
Me_{trans} [a])	17.3	1.09	–	1.03	1.03; 4.53; 7.96
Me_{cis} [a])	24.1	1.03	–	1.09	1.09; 7.48; 7.96
OH	–	7.96	–	–	1.03; 1.09; 4.53; 7.48

[a]) Me_{cis} and Me_{trans} mean that the Me groups are *cis* and *trans*, respectively, to the pyridinyl group.

Table 2. *^{1}H- and ^{13}C-NMR Chemical Shifts for* **1b** *at 300 K, Including HMQC* (^1J(C,H)), *HMBC* (^nJ(C,H), n = 2, 3), *and NOESY Correlations.* In (D_6)DMSO.

	HMQC		HMBC		NOESY
	δ(C)	δ(H)	^2J(C,H)	^3J(C,H)	^{1}H,^{1}H
H–C(2)	88.7	4.54	–	–	1.07; 7.89; 8.57
C(4), C(5)	66.7	–	1.04; 1.07	1.04; 1.07	–
H–C(2′)	149.0	8.57	–	7.82; 8.42	4.54; 7.89
C(3′)	136.5	–	–	7.36	-
H–C(4′)	137.6	7.82	–	8.42; 8.57	1.04; 7.36
H–C(5′)	123.5	7.36	–	–	7.82; 8.42
H–C(6′)	150.2	8.42	–	7.82; 8.57	7.36
Me_{trans} [a])	17.7	1.07	–	1.04	1.04; 4.54; 7.89
Me_{cis} [a])	24.7	1.04	–	1.07	1.07; 7.82; 7.89
OH	–	7.89	–	–	1.04; 1.07; 4.54; 8.57

[a]) Me_{cis} and Me_{trans} mean that the Me groups are *cis* and *trans*, respectively, to the pyridinyl group.

The NOESY data for **1b** (*Table 2*) establish that H–C(2) correlates with H–C(2′) and with the Me groups *trans* to the pyridinyl group (Me_{trans}) and also that H–C(4′)

correlates with the Me groups *cis* to the pyridinyl group (Me_{cis}). This indicates a preference for one rotamer in **1b**. By extension, only two identical rotamers are expected for **1a**. From the spatial dispositions of the substituent groups at the imidazolidine ring obtained by 2D NMR, conformational-analysis calculations of **1a** and **1b** were made. The same procedure was adopted for compound **1c** (see below). As explained in the *Sect. 3*, a comprehensive conformational search was carried out at the HF/3-21G(d) level. All possible spatial orientations of the OH groups (as specified by the *Formulae* given in *Table 3*) and also rotations of the pyridinyl group around the single bond were investigated. The relative *Gibbs* energies, thermal corrections, and gas-phase-energy differences are given in *Table 3* for **1a**–**c**. The lowest-energy geometries obtained from the calculations show the pyridinyl groups to be equatorial and the Me groups to be both axial (Me_{ax}) and equatorial (Me_{eq}) at the imidazolidine ring. *Figs. 2–4*, show the HF/6-31G(d) fully optimized structures (global minima) for **1a**, **1b**, and **1c**, respectively. We first discuss the conformations of **1a** and **1b**, leaving **1c** for later.

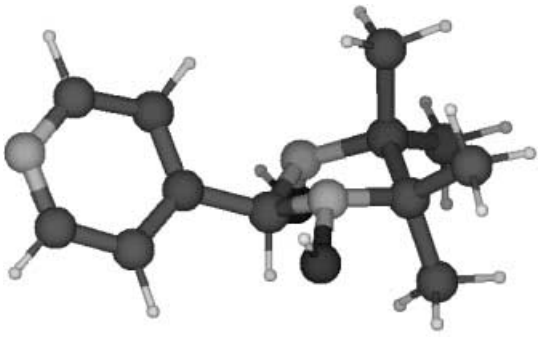

1a-I

Fig. 2. *HF/6-31G(d) Fully optimized structure of the global minimum located on the PES for* **1a**

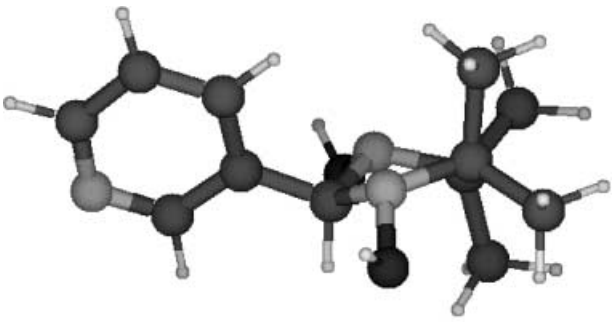

1b-I

Fig. 3. *HF/6-31G(d) Fully optimized structure of the global minimum located on the PES for* **1b**

According to the literature, *Van der Waals* repulsions are reduced for staggered axial and equatorial Me groups, relative to eclipsed Me groups [17]. Also, it is known

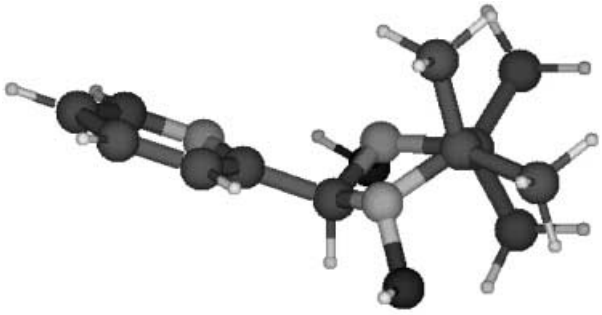

1c-I

Fig. 4. *HF/6-31G(d) Fully optimized structure of the global minimum located on the PES for* **1c**

Table 3. *Electronic- Plus Nuclear-Repulsion-Energy Differences in the Gas Phase* $\Delta E_{ele\text{-}nuc}$ [kcal mol^{-1}], *Thermal-Energy Corrections* ΔG_T [kcal mol^{-1}] *and* Gibbs *energy differences* ΔG [kcal mol^{-1}] *for the Structures* **1a**–**1c**. *T* 298.15 K, *p* 1 atm. The labels **I**–**III** stand for the distinct relative orientation of the two OH groups in relation to the pyridinyl group, as shown below for **1c-I**; both OH opposite to pyridinyl; **II** the two OH opposite to each other; **III** both OH on the same side as pyridinyl.

	$\Delta E_{ele\text{-}nuc}$ (HF/3-21G(d))	ΔG_T (HF/3-21G(d))	ΔG[a]) (HF/3-21G(d))
1a-I[b])[c])	0.0	0.0	0.0
1a-II[b])[d])	10.3	– 0.8	9.4
1a-III[b])	8.4	– 0.4	7.9
1b-I[b])[c])	0.0	0.0	0.0
1b-II[b])	6.9	– 0.1	6.7
1b-III[b])	4.3	– 0.8	3.5
1c-I[e])	0.0	0.0	0.0
1c-I′[f])	4.58	– 0.62[j])	3.96
1c-I″[g])	3.00	– 0.77[j])	2.23
1c-II[b])[h])	2.11	0.15[j])	2.26
1c-III[b])[i])	9.15	0.07[j])	9.22

[a]) $\Delta G = \Delta E_{ele\text{-}nuc} + \Delta G_T$. [b]) Rotation of the pyridinyl group around the single bond did not change significantly the relative energy values. [c]) The dihedral angle between the pyridinyl and imidazolidine N-atoms for **1a-I** is 119° (HF/6-31G(d) value = 152°). [d]) The dihedral angle between the pyridinyl and imidazolidine N-atoms for **1b-I** is 68° (HF/6-31G(d) value = 104°). [e]) The dihedral angle between the pyridinyl and imidazolidine N-atoms (wN–C–C–N) is 50° (HF/6-31G(d) value = 43°). [f]) w(N–C–C–N) = – 50° (HF/6-31G(d) value = – 54°). [g]) w(N–C–C–N) = 173° (HF/6-31G(d) value = 168°). [h]) w(N–C–C–N) = 53° (HF/6-31G(d) value = 83°). [i]) w(N–C–C–N) = 113° (HF/6-31G(d) value = 103°). [j]) The corresponding HF/6-31G(d) values for structures **1c-I′**, **1c-I″**, **1c-II**, and **1c-III** are: – 0.42, – 0.39, – 0.19, and 0.08 kcal mol^{-1}, resp.

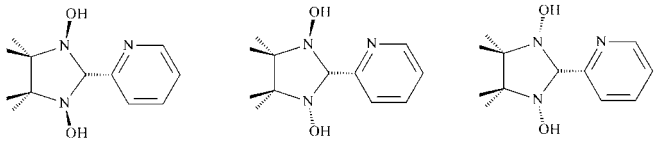

1c-I **1c-II** **1c-III**

that equatorial Me groups in cyclic systems show larger ^{1}H-NMR chemical shifts than axial Me groups, while the opposite behavior is observed for the corresponding ^{13}C-NMR chemical shifts [18]. This was confirmed by ACD calculations and by the HMQC correlation [3]. However, one can anticipate that the Me groups will be influenced not only by their axial or equatorial positions, but also by the OH O-atoms and/or the pyridinyl group. In addition, we find that $Me_{ax,trans}$ and $Me_{eq,trans}$ are in the same magnetic environment, and also $Me_{ax,cis}$ and $Me_{eq,cis}$, presumably because of the rapid flexure of the imidazolidine ring.

NOESY verified that only the more-shielded Me groups correlate with H–C(3′)/H–C(5′) in the spectrum of **1a** and with H–C(4′) in that of **1b**, indicating that these more-shielded Me groups are *cis* to the pyridinyl group (Me_{cis}). *Table 4* presents the interatomic distances calculated for the HF/6-31G(d)-optimized geometries of **1a** and **1b**, and *Table 5* gives the relevant dihedral angles. For instance, in the case of **1a**, the shorter interatomic distances between H–C(2) and both $Me_{ax,trans}$ (2.24 Å) and $Me_{eq,trans}$ (3.72 Å) in relation to the Me_{cis} groups (4.15 and 4.60 Å, resp.) agree with this NOESY correlation. In contrast, the two resonance signals obtained for the four Me groups can be attributed to their differing distances from the OH groups. Because $Me_{ax,trans}$ (2.78 Å) and $Me_{eq,trans}$ (2.49 Å) lie closer to the O-atoms than $Me_{ax,cis}$ (3.94 Å) and $Me_{aq,cis}$ (3.29 Å), one expects and observes more shielding by the O-atoms of these axial Me groups, and hence larger ^{1}H-NMR chemical shifts. Similar results are found for **1b**. In fact, δ(H) is 1.09 for Me_{trans} of **1a** and δ(H) 1.07 for Me_{trans} of **1b** *vs.* δ(H) 1.03 and 1.04 for the corresponding Me_{cis} groups. The corresponding Me C-atom show shift changes of opposite sign, because of the γ-effect of the OH groups.

Table 4. *HF/6-31(d)-Optimized Interatomic Distances* [Å], *Calculated for Methyl H-Atoms*

	$Me_{ax,trans}$ [a])	$Me_{eq,trans}$ [a])	$Me_{ax,cis}$ [a])	$Me_{eq,cis}$ [a])
1a-I: H–C(2)	2.24	3.72	4.15	4.60
*O*H–N(1)	2.78	2.49	4.01	5.14
*O*H–N(3)	3.18	4.91	3.94	3.29
1b-I: H–C(2)	3.65	2.21	4.60	4.19
*O*H–N(1)	2.49	3.18	3.29	3.96
*O*H–N(3)	4.89	2.87	5.15	4.00

[a]) Me_{cis} and Me_{trans} mean that the Me groups are *cis* and *trans*, respectively, to the pyridinyl group.

Table 5. *Relevant Dihedral Angles for the Fully Optimized HF/6-31(d) Main Equilibrium Structures Located on the PES for the* **1a** and **1b** *species.* The labels are specified in *Fig. 1.*

1a-I:	H–O–N(3)–C(2)	120.3	$Me_{ax,trans}$–C(5)–N–C(2)	– 72.4
	H–O–N(1)–C(2)	– 117.4	$Me_{eq,trans}$–C(4)–N–C(2)	136.6
	C(5′)–C(4)–C(2)–N(3)	152.3	$Me_{ax,cis}$–C(4)–N–C(2)	– 105.3
	O–N(3)–C(2)–C(4′)	– 101.1	$Me_{eq,cis}$–C(5)–N–C(2)	166.8
	O–N(1)–C(2)–C(4′)	76.4		
1b-I:	H–O–N(1)–C(2)	116.3	$Me_{ax,trans}$–C(4)–N–C(2)	– 133.7
	H–O–N(3)–C(2)	– 119.3	$Me_{eq,trans}$–C(5)–N–C(2)	72.2
	C(2′)–C(3′)–C(2)–N(1)	103.8	$Me_{ax,cis}$–C(5)–N–C(2)	– 162.7
	O–N(1)–C(2)–C(3′)	– 75.1	$Me_{eq,cis}$–C(4)–N–C(2)	108.2
	O–N(3)–C(2)–C(3′	97.5		

The data of *Table 4* show that each of the four Me groups has different distances to the two OH groups. However, only single chemical shifts are observed for $Me_{ax,trans}$/$Me_{eq,trans}$ (δ(H) 1.09 (**1a**) or 1.07 (**1b**)), and also for $Me_{ax,cis}$/$Me_{eq,cis}$ (δ(H) 1.03 (**1a**) and 1.04 (**1b**)) Thus, conformational averaging *via* pseudorotation of the imidazolidine ring must take place. This necessitates a rapid axial–equatorial inversion of the Me groups, and a relatively low energy barrier. In fact, several pentacyclic systems have an axial–equatorial interconversion energy barrier of *ca.* 20 kJ/mol [19], this being dependent on the substitutent groups [20]. For this reason, all the structures discussed below require mirror-image structures to be equally present. These are not treated as distinct conformations in the discussion that follows.

With isomer **1c**, 1D (^{1}H- and ^{13}C-NMR) and 2D (HMQC, HMBC, and NOESY) spectra were also obtained in the temperature range of 290 to 380 K. *Fig. 5* presents partial ^{1}H-NMR spectra of **1c** in the region of the Me signals (δ(H) 1.00–1.15) at different temperatures (290–380 K). Two Me signals cross at 300 K without evident exchange broadening. These results are interesting because they suggest that more than one distinct and thermally accessible conformation is present.

To investigate the ^{1}H-NMR profile shown in *Fig. 5*, a complete conformational analysis was carried out for isomer **1c** at the HF/6-31G(d) level of calculation[1]). The position of the OH groups was allowed to vary, and also rotation of the pyridinyl group around the single bond was performed. In addition, the transition-state (TS) structures connecting the plausible minima located on the PES were found, and hence the barriers for conformational interconversion could be calculated. A summary of the calculations is reported in *Table 6*[1]). There is only one thermally accessible conformation for **1a** and **1b** (data not shown since the relative energies are too high). However, for **1c**, three conformations have relative percentage concentrations above the NMR experimental limit of detection (*ca.* 5%), namely **1c-I**, **1c-I″**, and **1c-II**. The HF/6-31G(d)-optimized structures for **1c-I″** and **1c-II** are given in *Figs. 6* and *7*, respectively, and the corresponding calculated interatomic distances and relevant dihedral angles in *Tables 7* and *8*, respectively. It can also be seen that structure **1c-I** is not altogether predominant in the temperature range investigated (290–380 K).

The assignments of the ^{1}H- and ^{13}C-NMR data of **1c** at 290 K were confirmed by the HMQC correlations and also by HMBC and NOESY data (*Table 9*). Differently from the results obtained for **1a** and **1b**, the HMQC data show that for the Me groups of **1c** at 290 K, the H-atoms of smaller chemical shifts (δ(H) 1.06) correlate with the C-atoms with smaller chemical shifts (δ(C) 17.5). This probably implies additional contributions to the ^{1}H-NMR chemical shifts. The less-shielded Me signals (δ(H) 1.07) correspondingly correlate with the C-atoms of larger chemical shift (δ(C) 24.2). Also, the NOESY of **1c** at 290 K correlates H–C(2) at δ(H) 4.64 with the Me groups having the smaller chemical shift, δ(H) 1.06 (*Table 9*), opposite to the situation observed for **1a** and **1b**. This cannot indicate a different imidazolidine-ring conformation as compared to **1a** and **1b** because all the other NOESY correlations are similar. The theoretical results reported in *Table 6* also show that structure **1c-I** is the global minimum on the PES and similar to **1a** and **1b**, except for a rotation of the pyridinyl group that separates H–C(2) from H–C(3′). In addition, no interannular rotamer favors a close approach between

[1]) The full results can be obtained as supplementary material directly from the authors.

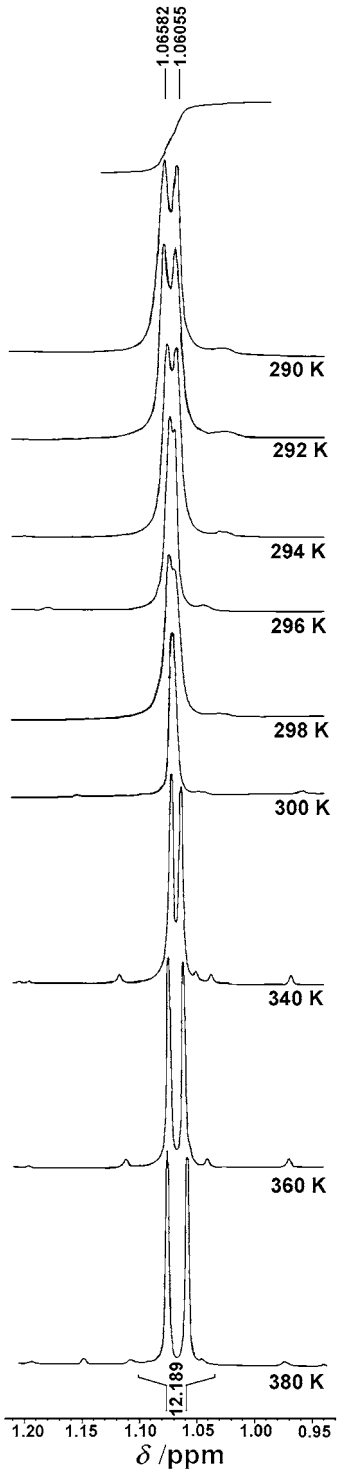

Fig. 5. *Partial ^{1}H-NMR spectra of* **1c** *in the Me region δ(H) 1.00–1.15, at different temperatures.* At 400 MHz, in (D_6)DMSO with $SiMe_4$ as internal standard.

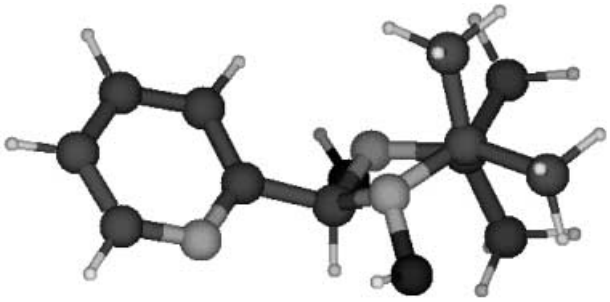

1c-I″

Fig. 6. *HF/6-31G(d) Fully optimized structure of* **1c-I″**

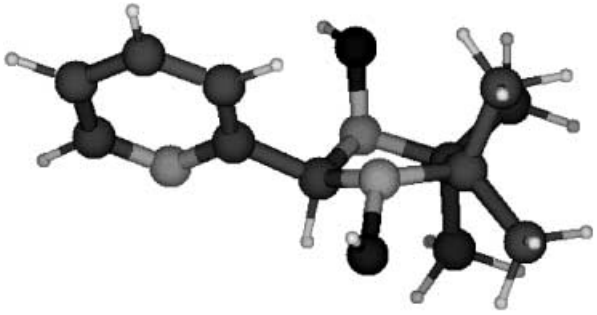

1c-II

Fig. 7. *HF/6-31G(d) Fully optimized structure of* **1c-II**

H−C(2) and H−C(3′) in **1c-I**. It is interesting to note from *Fig. 4* that there is an intramolecular H-bond between the pyridinyl N-atom and the OH H-atom ($d_{(N\cdots H)}$ = 2.3 Å). This significantly stabilizes the **1c-I** structure.

Table 10 presents ^{1}H- and ^{13}C-NMR data for **1c** at 300 K, confirmed by the HMQC correlations, and also HMBC and NOESY data. At this temperature, the ^{1}H-NMR Me signals overlap, but the corresponding ^{13}C-NMR signals do not. Hence the overlap must be accidental. The NOESY experiment of **1c** at 300 K confirms that H−C(2) (δ(H) 4.66) correlates with OH (δ(H) 7.75) and does not correlate with H−C(3′) (δ(H) 7.60). Therefore, the pyridinyl N-atom is spatially near H−C(2), and there is restricted interannular rotation, similarly to **1a**, **1b**, and **1c** at 290 K. The correlation between H−C(3′) and OH indicates that the imidazolidine ring of **1c** at 300 K has conformational properties similar to those of **1a** and **1b**. Structure **1c-I** in *Fig. 4* meets these requirements. Structure **1c-I″** in *Table 6*, with its altered inter-ring angle, is also thermally accessible and can, therefore, explain the unusual thermal variation of the Me δ(H), *via* the angular dependence of the shifts induced by the pyridinyl ring current.

Table 6. *Thermal-Energy Correction* ($\Delta G_T = \Delta E_{int} - T\Delta S$), *Solvation-Energy Contribution* (ΔE^{solv}), *and* Gibbs *Energy Including the Solvent Effect* (DMSO) *through the PCM Continuum Model* ($\Delta G^{solv} = \Delta E^{gas}{}_{ele\text{-}nuc} + \Delta G_T + \Delta E^{solv}$) *for the Equilibrium Structures Located on the PES for the* **1c** *Species*. The calculations were made relative to the lowest-energy structure **1c-I**. All calculations were performed with fully optimized HF/6-31G(d) equilibrium structures.

		HF/6-31G(d) Thermal energy ΔG_T[a]) [kcal mol^{-1}]	MP2/6-31G(d,p) Solvation energy ΔE^{solv}[b]) [kcal mol^{-1}]	MP2/6-31G(d,p) [$\Delta E_{ele\text{-}nuc}$ *Term*] ΔG^{sol} [kcal mol^{-1}]	MP2/6-31G(d,p) Concentration [%][c])
T 290 K, $p = 1$ atm:	**1c-I**	0.0 (0.0)	0.0	0.0	81.4
	1c-I′	−0.41 (0.01)	−0.18	2.83	0.6
	1c-I″	−0.38 (0.03)	−0.58	1.09	12.3
	1c-II	−0.18 (0.11)	−1.46	1.53	5.7
	1c-III[d])	0.082 (0.17)	−1.65	6.33	< 0.1
T 300 K, p 1 atm:	**1c-I**	0.0 (0.0)	0.0	0.0	80.2
	1c-I′	−0.42 (0.01)	−0.18	2.82	0.7
	1c-I″	−0.39 (0.03)	−0.58	1.08	12.9
	1c-II	−0.19 (−0.73)	−1.46	1.52	6.2
	1c-III[d])	0.081 (0.17)	−1.65	6.33	< 0.1
T 350 K, p 1 atm:	**1c-I**	0.0 (0.0)	0.0	0.0	72.9
	1c-I′	−0.49 (0.06)	−0.18	2.75	1.5
	1c-I″	−0.45 (0.07)	−0.58	1.02	16.8
	1c-II	−0.24 (1.09)	−1.46	1.47	8.8
	1c-III[d])	0.079 (0.13)	−1.65	6.33	< 0.1
T 380 K, p 1 atm:	**1c-I** (350 K)	0.0	0.0	0.0	69.1
	1c-I′ (350 K)	−0.53	−0.18	2.71	1.9
	1c-I″ (350 K)	−0.49	−0.58	0.98	18.9
	1c-II (300 K)	−0.26	−1.46	1.45	10.1
	1c-III (290 K)[d])	0.078	−1.65	6.33	< 0.1

[a]) The ΔG_T^{corr} (neglecting the low-frequency mode) values are in parenthesis. [b]) The corresponding HF/6-31G(d,p) ΔE^{solv} values for the **1c-I′**, **1c-I″**, **1c-II**, and **1c-III** structures are: −0.19, −0.62, −1.42, and −1.55 kcal mol^{-1}, resp. [c]) Possible species to be found in equilibrium: **I**, **I′**, **I″**, and **II**; $R = 1.986218511 \cdot 10^{-3}$ kcal/mol·K; calculation of equilibrium constants: $[\mathbf{II}]/[\mathbf{I}] = \exp(-\Delta G_{\mathbf{II}}/RT)$; $[\mathbf{I'}]/[\mathbf{I}] = \exp(-\Delta G_{\mathbf{I'}}/RT)$; $[\mathbf{I''}]/[\mathbf{I}] = \exp(-\Delta G_{\mathbf{I''}}/RT)$; $[\mathbf{II}] + [\mathbf{I}] + [\mathbf{I'}] + [\mathbf{I''}] = 1$; $[\mathbf{I}] = 1/[(1 + \exp(-\Delta G_{\mathbf{II}}/RT) + \exp(-\Delta G_{\mathbf{I'}}/RT) + \exp(-\Delta G_{\mathbf{I''}}/RT)]$. [d]) Rotation of the pyridinyl group was performed but the energy and thermal correction results did not change significantly.

Table 7. *HF/6-31(d)-Optimized Interatomic Distances* [Å], *Calculated for Methyl H-Atoms*

		$Me_{ax,trans}$ [a])	$Me_{eq,trans}$ [a])	$Me_{ax,cis}$ [a])	$Me_{eq,cis}$ [a])
1c-I:	H–C(2)	4.03	2.48	4.65	4.00
	*O*H–N(1)	4.91	3.08	3.34	3.90
	*O*H–N(3)	2.46	2.48	5.08	4.05
1c-I′:	H–C(2)	2.31	2.31	4.61	4.08
	*O*H–N(1)	3.18	3.18	3.30	3.91
	*O*H–N(3)	2.65	2.65	5.12	4.00
1c-I″	H–C(2)	3.90	2.36	4.64	4.08
	*O*H–N(1)	4.92	3.14	3.34	4.02
	*O*H–N(3)	2.46	2.59	5.11	3.93
1c-II	H–C(2)	3.38	2.14	4.63	4.31
	*O*H–N(1)	4.90	4.09	2.44	2.46
	*O*H–N(3)	2.53	3.19	5.14	3.92
1c-III	H–C(2)	3.83	2.28	4.69	4.22
	*O*H–N(1)	4.95	4.08	2.44	2.32
	*O*H–N(3)	3.48	4.01	4.86	2.98

[a]) Me_{cis} and Me_{trans} mean that the Me groups are *cis* and *trans*, respectively, to the pyridinyl group.

Table 8. *Relevant Dihedral Angles for the Fully Optimized HF/6-31(d) Main Equilibrium Structures Located on the PES for the* **1c** *Species*. The labels are specified in *Fig. 1*.

	H–O–N(3)–C(2)	H–O–N(1)–C(2)	N–C(2′)–C(2)–N(3)	O–N(3)–C(2)–C(2′)	O–N(1)–C(2)–C(2′)
1c-I	86.1	– 127.6	43.4	– 86.7	116.6
1c-I′	118.6	– 123.6	– 59.3	– 79.3	105.9
1c-I″	121.3	– 103.9	167.5	– 83.3	107.7
1c-II	– 114.8	111.0	102.8	36.6	1.4
1c-III	– 117.3	– 119.8	83.3	46.4	88.1
	$Me_{ax,trans}$–C(5)–N–C(2)	$Me_{eq,trans}$–C(4)–N–C(2)	$Me_{ax,cis}$–C(4)–N–C(2)	$Me_{eq,cis}$–C(5)–N–C(2)	
1c-I	– 147.9	77.4	– 161.8	94.5	
1c-I′	– 140.8	73.4	– 165.7	101.2	
1c-I″	– 142.7	74.4	– 164.7	99.5	
1c-II	– 123.2	82.2	– 161.6	118.8	
1c-III	– 144.5	81.2	– 161.9	96.0	

Table 11 presents ^{1}H- and ^{13}C-NMR data for **1c** at 350 K, confirmed by the HMQC correlations, and also HMBC and NOESY data. NOESY Analyses indicate correlation of H–C(2) (δ(H) 4.73) with the Me_{trans} of larger chemical shifts (δ(H) 1.13) and of H–C(3′) (δ(H) 7.61) with the Me_{cis} of smaller chemical shifts (δ(H) 1.11). The OH signal is much broader (width >50 Hz) than in the other spectra. This prevents the detection of NOESY correlations with other H-atoms in the molecule. However, the similarities of the correlations among the other types of H-atoms present in this substance at this temperature, and those verified in NMR spectra of **1a** and **1b**, suggest that the OH groups at the imidazolidine ring of **1c** at 350 K are also *trans* to the

Table 9. *^{1}H- and ^{13}C-NMR Chemical Shifts for* **1c** *at 290 K, Including HMQC* (^1J(C,H)), *HMBC* (^nJ(C,H), $n=2, 3$), *and NOESY Correlations.* In (D_6)DMSO.

	HMQC		HMBC		NOESY
	δ(C)	δ(H)	^2J(C,H)	^3J(C,H)	^{1}H,^{1}H
H–C(2)	91.5	4.64	–	7.62	1.06; 7.75
C(4), C(5)	66.4	–	1.06; 1.07	1.06; 1.07	–
C(2′)	161.6	–	–	7.75; 8.47	–
H–C(3′)	122.7	7.62	7.75	4.64; 7.27	1.07; 7.75
H–C(4′)	136.2	7.75	7.27; 7.62	8.47	7.27; 7.62
H–C(5′)	122.5	7.27	7.75; 8.47	7.62	7.75; 8.47
H–C(6′)	148.1	8.47	7.27	7.75	7.27
Me_{trans}[a])	17.5	1.06	–	1.07	1.07; 4.64; 7.75
Me_{cis}[a])	24.2	1.07	–	1.06	1.06; 7.62; 7.75
OH	–	7.75	–	–	1.06; 1.07; 4.64; 7.62

[a]) Me_{cis} and Me_{trans} mean that the Me groups are *cis* and *trans*, respectively, to the pyridinyl group.

Table 10. *^{1}H- and ^{13}C-NMR Chemical Shifts for* **1c** *at 300 K, Including HMQC* (^1J(C,H)), *HMBC* (^nJ(C,H), $n=2, 3$), *and NOESY Correlations.* In (D_6)DMSO.

	HMQC		HMBC		NOESY
	δ(C)	δ(H)	^2J(C,H)	^3J(C,H)	^{1}H,^{1}H
H–C(2)	91.9	4.66	–	7.75	1.06; 7.75
C(4), C(5)	66.8	–	1.06	1.06	–
H–C(2′)	161.9	–	–	7.75; 8.46	–
H–C(3′)	123.1	7.60	7.75	4.66; 7.25	1.06; 7.75
H–C(4′)	136.5	7.75	7.25; 7.60	8.46	7.25; 7.60
H–C(5′)	122.9	7.25	7.75; 8.46	7.60	7.75; 8.46
H–C(6′)	148.5	8.46	7.25	7.75	7.25
Me_{cis}/Me_{trans}[a])[b])	17.9	1.06	–	–	4.66; 7.60; 7.75
Me_{trans}/Me_{cis}[a])[c])	24.6	1.06	–	–	4.66; 7.60; 7.75
OH	–	7.75	–	–	1.06; 4.66

[a]) Me_{cis} and Me_{trans} mean that the Me groups are *cis* and *trans*, respectively, to the pyridinyl group. [b]) *cis* and vicinal to OH–N(1) and OH–N(3), respectively. c) *trans* and vicinal to OH–N(1) and OH–N(3), respectively.

pyridinyl group. This interpretation is supported by the theoretical conformational analysis, for the two lowest-energy structures have the OH groups *trans* to pyridinyl.

Thus, although the NMR results for **1c** at 350 K are not sufficient to reach definitive conclusions on the existence of a third distinct conformation such as **Ic-II** (*Fig. 7*), the theoretical calculations provide useful information on the possible equilibrium conformations.

5. Conclusions. – In the present work, NMR data show how the differently attached pyridinyl groups affect the conformation of the 1,3-dihydroxy-4,4,5,5-tetramethyl-2-pyridinylimidazolidines **1.** Both **1a** and **1b** have a single conformation with the two OH substituents *trans* to the pyridinyl group over the temperature range 290 to 380 K. In

Table 11. *^{1}H- and ^{13}C-NMR Chemical Shifts for* **1c** *at 350 K, Including HMQC* (^1J(C,H)), *HMBC* (^nJ(C,H), $n = 2, 3$), *and NOESY Correlations.* In (D_6)DMSO.

	HMQC		HMBC		NOESY
	δ(C)	δ(H)	^2J(C,H)	^3J(C,H)	^{1}H,^{1}H
H–C(2)	90.8	4.73	–	7.73	1.13
C(4), C(5)	66.2	–	1.11; 1.13	1.11; 1.13	–
C(2′)	161.1	–	–	7.73; 8.48	–
H–C(3′)	122.0	7.61	7.73	4.73; 7.23	7.73; 1.11
H–C(4′)	135.3	7.73	7.23; 7.61	8.48	7.61
H–C(5′)	121.9	7.23	7.73; 8.48	7.61	8.48; 7.73
H–C(6′)	147.5	8.48	7.23	7.73	7.23
Me_{trans}[a])	17.1	1.13	–	1.11	4.73
Me_{cis}[a])	23.5	1.11	–	1.13	7.61
OH	–	7.40	–	–	–

[a]) Me_{cis} and Me_{trans} mean that the Me groups are *cis* and *trans*, respectively, to the pyridinyl group.

contrast, for **1c**, two conformations can be proposed to exist in this temperature range, having different rotations of the pyridinyl group (around the single bond) with respect to the imidazolidine ring. At 290 K, the OH groups and the pyridinyl substituent are again *trans* but have a H-bond between the OH H-atom and the pyridinyl N-atom. At 300–350 K, the spatial disposition of the OH groups remains similar, but a second conformation gains importance as the H-bond weakens, with its pyridinyl group almost perpendicular to the imidazolidine ring. The 350 K data confirm that the two OH groups remain *trans* to the pyridinyl group, and so cannot confirm the existence of a third distinct conformation such as **1c-I′**. It should also be mentioned that the theoretical calculations provide useful information on the possible conformations that may exist in equilibrium and, therefore, help substantially to assign the experimental NMR data.

6. Supplementary Material. – The optimized coordinates of all structures discussed in the present work and the main structural parameters are available on request from the authors.

This research was supported by the *Brazilian Agencies CNPq* (*Conselho Nacional de Desenvolvimento Científico e Tecnológico*) and *FAPEMIG* (*Fundação de Amparo a Pesquisa do Estado de Minas Gerais*). We would like also to thank Prof. *Oliver W. Howarth* (Centre for NMR, Department of Chemistry, University of Warwick, England) for interesting suggestions and kindly proofreading the manuscript.

REFERENCES

[1] A. F. C. Alcântara, H. F. dos Santos, W. B. De Almeida, M. G. F. Vaz, L. M. M. Pinheiro, H. O. Stumpf, *Struct. Chem.* **1999**, *10*, 367; M. G. F. Vaz, L. M. M. Pinheiro, H. O. Stumpf, A. F. C. Alcântara, S. Golhen, L. Ouahab, O. Cador, C. Mathonière, O. Kahn, *Chem.–Eur. J.* **1999**, *5*, 1486; M. G. F. Vaz, M. Knobel, N. L. Speziali, A. M. Moreira, A. F. C. Alcântara, H. O. Stumpf, *J. Braz. Chem. Soc.* **2002**, *13*, 183.

[2] A. F. de C. Alcântara, D. Piló-Veloso, H. O. Stumpf, W. B. de Almeida, *Tetrahedron* **1997**, *53*, 16911.

[3] ACD/Labs Software, 133 Richmond St., W., Suite 605, Toronto, Ontario, Canada, M5 H 2L5.

[4] R. G. Parr, W. Yang, 'Density Functional Theory of Atoms and Molecules', Oxford University Press, New York, 1989.

[5] A. D. Becke, *Phys. Rev. A* **1988**, *38*, 3098; C. Lee, W. Yang, R. G. Parr, *Phys. Rev. B* **1993**, *37*, 785.

[6] R. Ditchfield, W. J. Hehre, J. A. Pople, *J. Chem. Phys.* **1971**, *54*, 724; W. J. Hehre, R. Ditchfield, J. A. Pople, *J. Chem. Phys.* **1972**, *56*, 2257.
[7] TITAN, *Wavefunction*, Inc., 18401 Von Karman, Suite 370, Irvine, CA 92612, USA, and *Schrödinger*, Inc., 1500 SW First Avenue, Suite 1180, Portland, OR 97201, USA.
[8] J. S. Binkley, J. A. Pople, W. J. Hehre, *J. Am. Chem. Soc.* **1980**, *102*, 939.
[9] M. J. Frisch, G. W. Trucks, H. B. Schlegel, G. E. Scuseria, M. A. Robb, J. R. Cheeseman, V. G. Zakrzewski, J. A. Montgomery, R. E. Stratmann, J. C. Burant, S. Dapprich, J. M. Millam, A. D. Daniels, K. N. Kudin, M. C. Strain, O. Farkas, J. Tomasi, V. Barone, M. Cossi, R. Cammi, B. Mennucci, C. Pomelli, C. Adamo, S. Clifford, J. Ochterski, G. A. Petersson, P. Y. Ayala, Q. Cui, K. Morokuma, D. K. Malick, A. D. Rabuck, K. Raghavachari, J. B. Foresman, J. Cioslowski, J. V. Ortiz, B. B. Stefanov, G. Liu, A. Liashenko, P. Piskorz, I. Komaromi, R. Gomperts, R. L. Martin, D. J. Fox, T. Keith, M. A. Al-Laham, C. Y. Peng, A. Nanayakkara, C. Gonzalez, M. Challacombe, P. M. W. Gill, B. G. Johnson, W. Chen, M. W. Wong, J. L. Andres, M. Head-Gordon, E. S. Replogle, J. A. Pople, 'Gaussian 98' (Revision A.6), Gaussian, Inc., Pittsburgh, PA, 1998.
[10] C. Møller, C. M. S. Plesset, *Phys. Rev.* **1934**, *46*, 618.
[11] J. W. Ochterski, in 'Thermochemistry in Gaussian', http://www.gausssian.com/thermo.htm, 2000.
[12] D. A. McQuarrie, J. D. Simon, 'Physical Chemistry, A Molecular Approach', University Science Books, Sausalito, 1997; D. A. McQuarrie, J. D. Simon, in 'Molecular Thermodynamics', University Science Books, Sausalito, 1999.
[13] H. F. Dos Santos, W. R. Rocha, W. B. De Almeida, *Chem. Phys.* **2002,** *280*, 31.
[14] M. Cossi, V. Barone, R. Camimi, J. Tomasi, *Chem. Phys. Lett*. **1996**, *255*, 327; V. Barone, M. Cossi, J. Tomasi, *J. Chem. Phys.* **1997**, *107*, 3210.
[15] W. B. De Almeida, H. F. Dos Santos, M. C. Zerner, *J. Pharm. Sci.* **1998**, *87*, 1101; H. F. Dos Santos, L. F. C. De Oliveira, S. O. Dantas, P. S. Santos, W. B. De Almeida, *Int. J. Quantum Chem.* **2000**, *80*, 1076.
[16] H. F. Dos Santos, M. V. De Almeida, W. B. De Almeida, *Theor. Chem. Acc*. **2002**, *107*, 229.
[17] G. I. Csonka, *J. Comput. Chem.* **1993**, *14*, 895; A. M. G. do Val, A. C. Guimarães, W. B. de Almeida, *J. Heterocycl. Chem*. **1995**, *32*, 557.
[18] E. L. Eliel, S. H. Wile, L. N. Mander, 'Stereochemistry of Organic Compounds', John Wiley & Sons, Inc., New York, 1994, p. 712; V. M. S. Gil, C. F. G. C. Geraldes, 'Ressonância Magnética Nuclear – Fundamentos, Métodos e Aplicações', Fund. Calouse Gulbenkian, Lisboa, 1987, p. 232; H. Friebolin, 'Basic One- and Two-Dimensional NMR Spectroscopy', VCH, Weinheim, 1993, p. 53.
[19] L. A. Carreira, G. J. Jiang, W. B. Person, J. N. Willis, *J. Chem. Phys.* **1972**, *56*, 1440.
[20] K. B. Wiberg, F. H. Walker, W. E. Pratt, J. Michl, *J. Am. Chem. Soc.* **1983**, *105*, 3638; M. P. Kozina, V. S. Mastryukov, E. M. Mil'vitskaya, *Russ. Chem. Rev.* **1982**, *51*, 765.

Received August 25, 2003